Spanwise Wake Structures of a Circular Cylinder and Two Circular Cylinders in Tandem

J. Wu
Department of Mechanical Engineering, Monash University, Clayton, Australia

L. W. Welch

M. C. Welsh
Division of Building Construction and Engineering, Commonwealth Scientific and Industrial Research Organization, Highett, Australia

J. Sheridan
Department of Mechanical Engineering, Monash University, Clayton, Australia

G. J. Walker
Department of Civil and Mechanical Engineering, University of Tasmania, Hobart, Australia

■ The structure of wakes downstream of cylinders is of major importance in the generation of flow-induced sound and vibration and also influences the convective heat transfer process. In particular, it is now thought that the formation of spanwise structures plays an important role. A better understanding of their development is required, and this could lead to ways of reducing both noise and vibration and to an improvement in heat and momentum transfer. Data are presented from tests carried out in a closed-circuit wind tunnel; also presented are data and flow visualizations from tests in a closed-circuit water tunnel. Hot-wire anemometer probes and pressure probes were used to measure velocity and pressure fluctuations at a number of spanwise locations in the wakes. From these measurements the spanwise coherence was calculated. The spanwise coherence increased as the distance between the cylinders in tandem was decreased; when this distance was less than three diameters, spanwise coherence at all spanwise separations was higher than for a single cylinder. Flow visualizations show the complex nature of the flow in the spanwise direction, particularly the existence of streamwise vortices. These appear to be responsible for the sharp reduction in spanwise coherence at large separations between the two cylinders in tandem. The work described is from a preliminary study with the object of developing a better understanding of near-wake flows prior to undertaking a comprehensive three-dimensional flow-field investigation.

Keywords: *spanwise coherence, vortex shedding, cylinders in tandem, wake, streamwise vortices*

INTRODUCTION

The wakes downstream of bluff bodies perform an important function in the generation of flow-induced sound and vibration and in the convective heat transfer process. Early investigations concentrated on the two-dimensional features of the wake, but it is now recognized that spanwise structures exist in the near wake. It is thought that these structures are significant in the transition to turbulence, heat and momentum transfer, and the development of flow-induced sound and vibration.

In previous efforts to understand the three-dimensional behavior of the wake flow, investigators [1–4] determined spanwise cross-correlation and coherence from pressure and velocity measurements in the wake behind stationary and vibrating circular cylinders. They found that when a cylinder was forced to oscillate at or near the natural Strouhal shedding frequency, the spanwise correlation length increased as the ratio of oscillation amplitude to cylinder diameter was increased. Sarpkaya [4] concluded that for flow past a cylinder at $Re = 1.9 \times 10^4$, increasing the ratio of oscillation amplitude to cylinder diameter from 0.05 to 0.10 increased the correlation length from $3.5D$ to $40D$ (D = cylinder diameter). Ramberg and Griffin [3], studying the spanwise correlation of velocity in a wake downstream of a vibrating cable, arrived at similar results for low flow velocities ($Re = 470–715$).

The spanwise coherence (correlation) is also influenced by the Reynolds number and free-stream turbulence. Kiya et al [2] studied a cylinder in a flow with a variety of free-stream turbulence levels and concluded that the spanwise cross-correlation length of the fluctuating surface pressure, if not solely controlled by the parameter $Re^{1.34}\ T$, is at least dependent on it. The Taylor number, T, characterizes the upstream turbulence intensity and the longitudinal integral scale of the free-stream turbulence [2]. They found that the spanwise correlation length decreased as this parameter increased.

Using a different approach, Arie et al [1], in a study with two circular cylinders in tandem, examined the effect of the spacing between cylinders on the spanwise correlation length. Their fluctuating pressure data, from pressure

Address correspondence to J. Wu, DBCE/CSIRO, P.O. Box 56, Highett, Vic 3190, Australia.

Experimental Thermal and Fluid Science 1994; 9:299–308

0894-1777/94/$7.00

tappings at 90° and 110° from the downstream stagnation point of the downstream cylinder, show a high spanwise correlation length when the separation gap between two cylinders is less than $2D$.

In the developed regions of the wake, the general form of the structure can be determined from time-history measurements on a plane normal to the free stream. Ferre et al. [5] and Hayakawa and Hussain [6] used hot-wire anemometer probes at multiple locations to obtain velocity data on the flow structures behind a cylinder. The former looked at the flow in the far wake; the latter, using an eduction method, investigated the large-scale coherent structures in the intermediate field, between $10D$ and $40D$.

The work described here is part of an experimental investigation of the spanwise structures in the near-wake region of bluff bodies using flow visualization techniques. It has been shown [7–9] that streamwise vortices are a predominant feature of the spanwise structures in the near wake. The streamwise vortices contribute to turbulence production and three-dimensionality in the near-wake region, leading to the formation of complex spanwise flow structures. It is our conjecture that these complex spanwise structures play a role in the wakes of cylinders in tandem.

In this study, the spanwise structures were detected using visualization techniques. Spanwise photographs and hot-wire data were obtained in the near wake of a single cylinder and two cylinders in tandem to demonstrate the three-dimensional flow structures.

WATER TUNNEL

General Description

The closed-circuit water tunnel was designed for low levels of free-stream turbulence in the 244 × 244 mm square working section. Water from the pump flowed through a straight measuring section containing a calibrated orifice plate and then through a diffuser into a settling chamber containing filters and a honeycomb straightening section. On leaving the settling chamber, the water passed through a two-dimensional 4-to-1 contraction, through a 660-mm-long duct, and into the 770-mm-long working section. The water leaving the working section flowed via a 440-mm-long duct into the outlet reservoir. The sections between the outlet of the contraction and the outlet reservoir were constructed from 20-mm acrylic sheet supported and joined by aluminum flanges. An observation window in the outlet reservoir permitted an on-axis view through the working section.

The mean flow velocity in the working section could be set between zero and a maximum of 400 mm/s. Between the wall boundary layers, the thickness of which is estimated to be 15 mm, the mean velocity profile was uniform within 0.5% and the longitudinal turbulence level was typically 0.1% when bandpass-filtered between 0.08 and 20 Hz. The spectrum of the fluctuating longitudinal velocity was free of sharp peaks and decreased in amplitude by 20 dB/Hz above 0.08 Hz.

The circular cylinders used in the water tunnel were 12 mm in diameter and were machined from acrylic. The models were normally mounted vertically and spanned the full (244 mm) height of the working section; no end plates were fitted.

Instrumentation and Flow Visualization

The low-frequency pressure fluctuations within the wake flow were measured using two solid-state pressure transducers (Micro Switch 163PC01D36), connected by PVC tubing to identical probes made from short lengths of 1.6-mm O.D. hypodermic tubing. The total length from probe tip to pressure transducer was less than 140 mm. The resulting signals were amplified by 40 dB and bandpassed between 0.01 and 10.0 Hz.

The fluctuating signals were recorded and processed on a DEC PDP 11/44 computer with two analog-to-digital converters operating through a laboratory peripheral accelerator. The fluctuating signals were typically sampled at 40 Hz for 320 s. A Data Precision four-channel Data 6000 universal waveform analyzer was used for signal monitoring and real-time statistical processing.

Local seeding of the flow with hydrogen bubbles was used for all flow visualization studies. The bubble stream was formed by electrolysis from an upstream nichrome wire (≈ 1 mm in diameter) cathode or from ribbon wires mounted flush with the surface of the models. A 4-W argon-ion laser and high intensity photographic floodlight were used to illuminate the bubble streams. The model and flow were viewed from three positions—from the side, from the end, and from downstream. The positions of the model, the hydrogen bubble stream, the plane of the laser light sheet (≈ 1 mm in thickness), and the camera are shown in Figs. 1a–c.

WIND TUNNEL

General Description

The tests in air were carried out in the 1200-mm-long, 600 × 600 mm square working section of a closed-circuit wind tunnel located at the University of Tasmania. The mean free-stream velocity through the working section could be increased to a maximum of 40 m/s. Between the wall boundary layers the mean velocity profile was uniform to within 1%, the variation in both yaw and pitch was within 0.5°, and the free-stream turbulence intensity was less than 0.15%. The thickness of the wall boundary layers is estimated to be approximately 50 mm.

The two 25.4-mm-diameter circular cylinder models were machined from aluminum. The cylinders were mounted in tandem in the vertical plane on the centerline of the tunnel and spanned the full width of the tunnel. The cylinders were fitted with 75-mm-diameter circular end plates located 400 mm apart. One of the cylinders was used in the single-cylinder tests.

Instrumentation

A DISA 55 M hot-wire anemometer was used to measure streamwise velocity fluctuations. The signals from the anemometer were typically bandpassed between 30 and 500 Hz and sampled at 1000 Hz for 10 s using an IBM PC computer fitted with a Metrabyte DAS-20 A/D converter. Subsequent data processing was carried out on the IBM PC using the Signal Technology signal processing software package ILS. The data were also monitored on an FFT analyzer, averaging the data from 200 FFT calculations.

The acoustic field across the working section was mapped

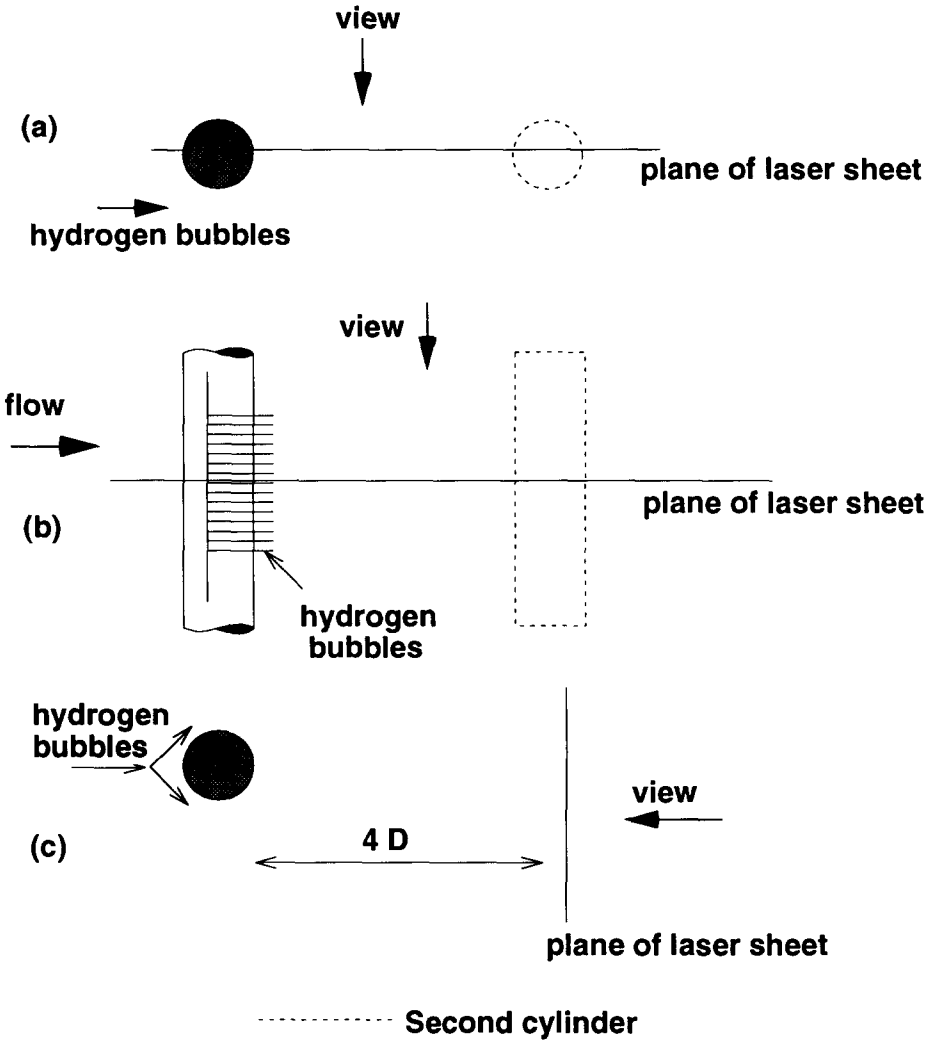

Figure 1. Positions of the model, the hydrogen bubble stream, the plane of laser light, and the camera for the photographs shown in the paper. (*a*) Side view; (*b*) end view; (*c*) downstream view. Direction of laser light: (*a*), (*b*) toward page; (*c*) from bottom to top.

using a Bruel & Kjar type 4138 microphone fitted with a nose cone to reduce noise produced by turbulence. The microphone was used to measure sound pressure levels. Particular attention was paid to identifying and avoiding flow velocities that could excite vibration or fluid-acoustic coupling modes within the tunnel or on the model [10]. An accelerometer mounted on the downstream cylinder, outboard of an end plate, was used to monitor vibration of the cylinder during the tests. The maximum rms acceleration was 2.1 mm/s^2, and the maximum rms displacement of 0.04 mm was insignificant with respect to the wake shedding [10].

The positioning and measurements of the cylinders and hot-wire probes located in the wind tunnel are shown in Fig. 2.

Experimental Uncertainty

Three factors contributed to the uncertainty associated with the hot-wire data presented in this paper: (1) the uncertainty in positioning of the probe ($< 0.4\%$ of cylinder diameter), (2) the uncertainty in the hot-wire probe calibration ($\approx 1.5\%$ free-stream velocity), and (3) the uncertainty in time mean of measurements of turbulent flow ($\approx 1\%$ of free-stream velocity). The overall uncertainty of the hot-wire data was approximately 2.0%, and the uncertainty of averaged coherence was approximately 2.1% at the 95% confidence level.

RESULTS

Coherence

The coherence of two velocity signals recorded at two points ΔZ apart along the span of the cylinder is defined by the equation

$$\mathrm{coh}(\Delta Z, \omega) = \frac{|G_Z(\omega)G^*_{Z+\Delta Z}(\omega)|}{\{[G_Z(\omega)G^*_Z(\omega)][G_{Z+\Delta Z}(\omega)][G^*_{Z+\Delta Z}(\omega)]\}^{1/2}} \quad (1)$$

Here $\mathrm{coh}(\Delta Z,\omega)$ is the coherence function depending on spanwise separation ΔZ and frequency ω; Z is the spanwise coordinate; G_Z and $G_{Z+\delta\Delta Z}$ are the Fourier transforms of the fluctuating velocity signals at Z and $Z + \Delta Z$; the asterisk denotes the complex conjugate. The Fourier transforms were obtained using FFT calculations. Typically 200 frames were used in averaging.

A coherence of unity corresponds to a full correlation at that particular frequency. Normally, the coherence

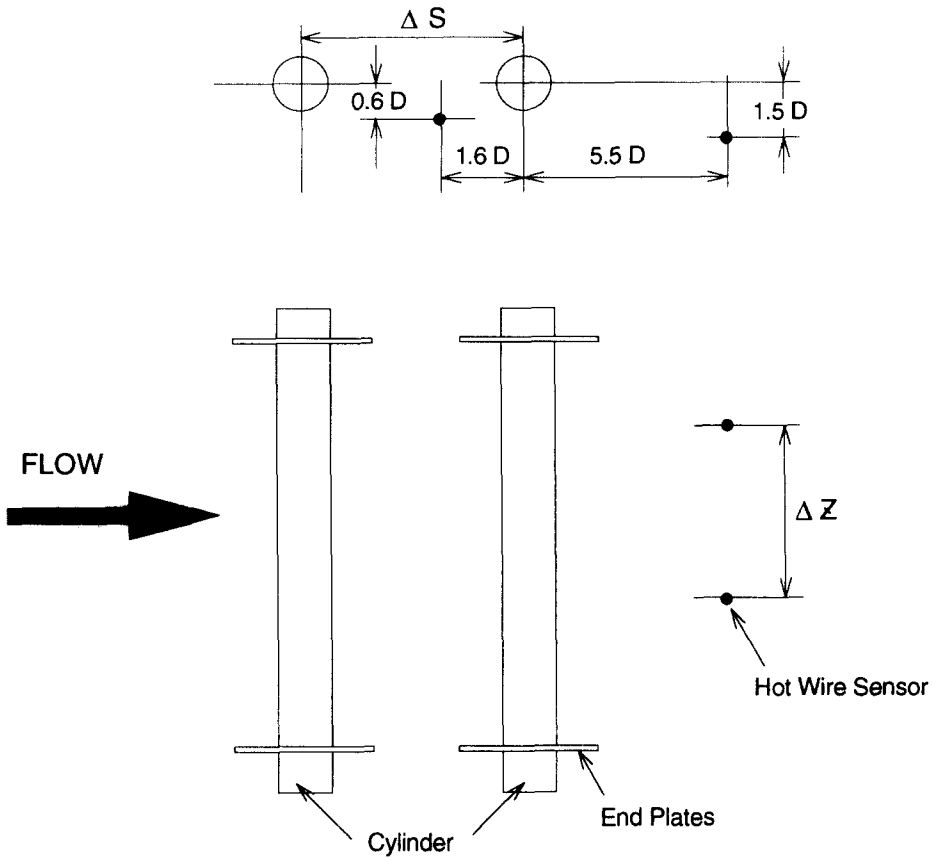

Figure 2. Test arrangement for the coherence measurement in a wind tunnel.

varies from 0 to 1. The coherence data produced in this paper are at the Strouhal vortex-shedding frequency.

The change in coherence at the shedding frequency with spanwise separation ΔZ of two cylinders in tandem, determined from measurements in the wind tunnel, is shown for a number of cylinder separation distances in Fig. 3. The coherence at the shedding frequency was determined from tests using two 25.4-mm-diameter cylinders at Re = 42,000 and 17,000. The data were derived from hot-wire probe measurements, with the probes positioned at the location shown in Fig. 3*a*. The coherence decreased with increasing spanwise separation of probes, and the rate of decrease increased when the separation distance between the cylinders, ΔS, was increased. Also plotted in Fig. 3*a* are data derived from measurements taken at the same location for a single cylinder. The decrease in coherence with spanwise separation for the single cylinder is similar to the decrease in the cross-correlation reported by Toebes [11]. When the separation between the two cylinders was $4D$ or less, then the coherence was always greater than for a single cylinder for the same spanwise separation. Data obtained from tests in the wind tunnel at Re = 17,000 are shown in Fig. 3*b*; the decrease in coherence with spanwise separation was less than for the higher flow velocity, but the trend was similar to that of the higher velocity data shown in Fig. 3*a*. Similar trends were found in the data obtained from the fluctuating pressure measurements for two 12-mm-diameter cylinders in the water tunnel at Re = 5000.

The variation of coherence with spanwise separation was also determined at a position between the cylinders (Fig. 4*a*). At this location it was found that when the cylinders were less than $3D$ apart, for all spanwise locations the coherence was greater than that of a single cylinder. When the spanwise separation was $4D$ or greater, then the decrease in coherence with spanwise separation was similar to that of a single cylinder. Similar trends were found at Re = 17,000 (Fig. 4*b*), but the rate of decrease of coherence with spanwise separation was less for cylinder separations greater than $3D$.

Figure 5 shows how the coherence (measured by two probes—one placed between the two cylinders and the other placed behind the downstream cylinder) of the velocity fluctuation decreases with increasing cylinder separation ΔS. The interference of the thermal wake of the upstream probe on the downstream probe was not important, as they were separated by the downstream cylinder. It was also found that the shedding frequency became lower when the separation between the cylinders was reduced (Fig. 6). The ratio of the shedding frequency when the cylinders were $3D$ apart to the shedding from a single cylinder was similar to the finding of Bull et al [12] for rectangular plates.

Flow Visualization

The flow visualization studies carried out in the water tunnel provided an opportunity to examine the developing structures either in real time or at slower speeds through video recording. The complexity of the developing near wake can be seen in photographs of structures behind a single cylinder (Fig. 7). The flow visualization arrangement is shown in Fig 1. Figure 7*a*, taken in the wake of a single cylinder, shows the vortex street when the hydrogen bub-

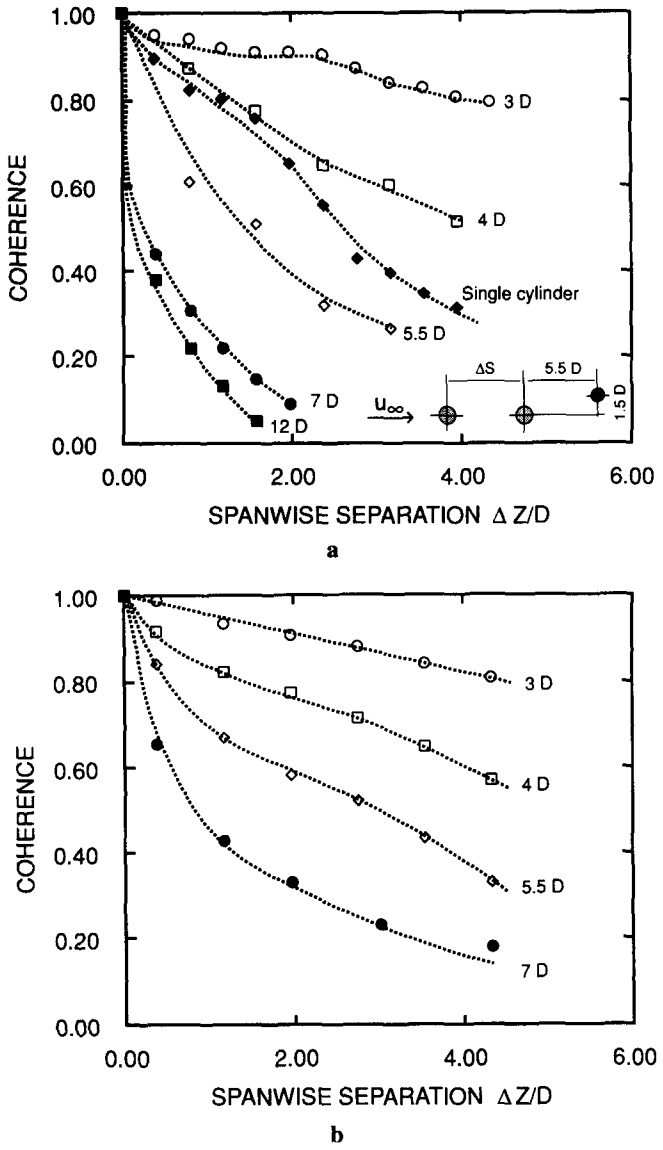

Figure 3. Spanwise coherence at shedding frequency; hot-wire probe data, downstream of two circular cylinders in tandem. ΔS denotes the spacing of the two cylinders in tandem. (*a*) Re = 42,000; D = 25.4 mm; $\Delta S = 3D$–$12D$. (*b*) Re = 17,000; 25.4 mm; $\Delta S = 3D$–$7D$.

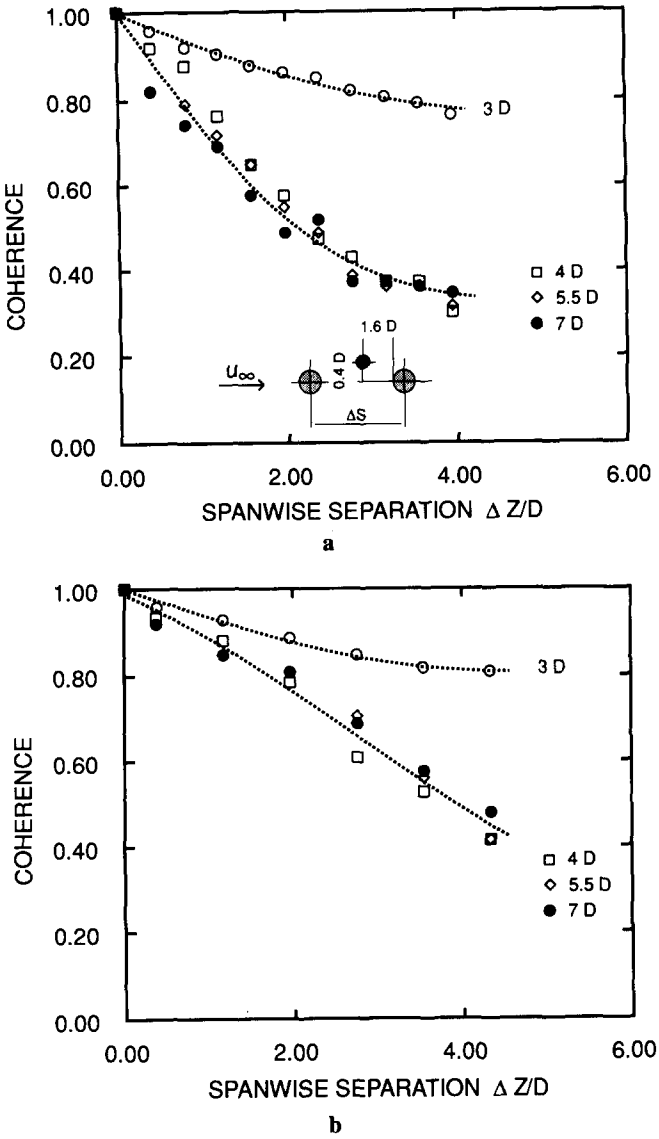

Figure 4. Spanwise coherence at shedding frequency; hot-wire probe data, between two circular cylinders in tandem. D = 25.4 mm, $\Delta S = 3D$–$7D$. (*a*) *Re* = 42,000; (*b*) *Re* = 17,000.

bles were generated from wires embedded in the surface of the cylinder at 45° either side of the upstream stagnation line. The developing spanwise structures can be seen in Figs. 7*b* and *c*. In Fig 7*b* (a side view of the cylinder), the bubbles were introduced upstream of the cylinder on a plane approximately 1 mm to one side of the centerline, while the plane of laser light was positioned in the centerline of the cylinder. The bubble stream in this photograph indicates pairs of counterrotating vortices on a plane at an angle to the upstream flow. In Fig 7*c* (a view from downstream looking upstream) the bubbles were introduced on the centerline upstream of the cylinder and the plane of laser light is normal to the mean flow direction at $4D$ downstream of the cylinder (Fig 7*c*). The plane of light cuts a developing spanwise Strouhal vortex structure in two places, as shown by a section across the wake at x–x (Fig. 7*a*), but with only the lower hydrogen bubble stream active. The mushroom-like structures outlined by the bubbles in Fig. 7*c* are indicative of counterrotating longitudinal vortices in the rib region of the spanwise vortex; the lower section of the bubbles shows the quasi-two-dimensional core of the spanwise vortex, or the Strouhal vortex. From the video sequences it was estimated that the ratio of the scale of the spanwise structure to that of the Strouhal vortex wake structures was about 0.5.

Typical vortex streets arising from two cylinders in tandem are shown in the end-view photographs of Fig. 8. From these it can be seen that when the separation is small, e.g., $\Delta S < 4D$, the formation of a vortex street behind the downstream cylinder is similar to that of the single cylinder (Fig. 7*a*). Also the shedding of the vortex from the upstream cylinder was suppressed (Figs. 8*a*, *b*).

When the distance between the cylinders was extended to $6D$, the Strouhal vortex formed behind the upstream

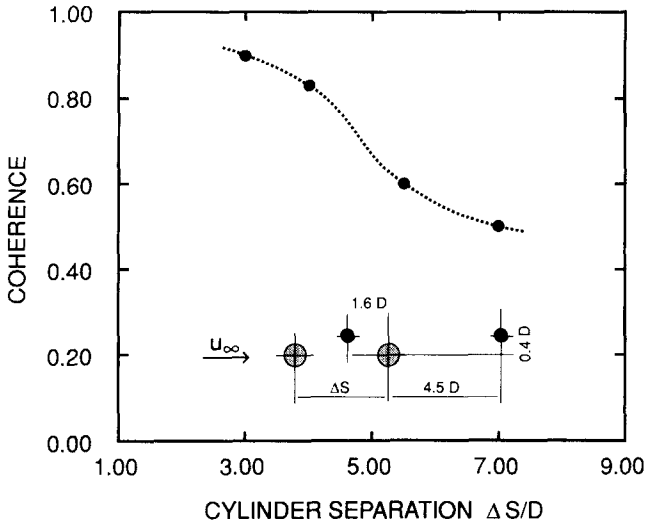

Figure 5. Coherence measured from two hot-wire probes placed in locations as shown. Re = 42,000; D = 25.4 mm.

cylinder as shown in Fig. 8*c*; the longitudinal vortices that were observed in the wake of the single-cylinder study could also be observed between the cylinders. Behind the downstream cylinder the vortex street became more chaotic due to the impingement of the *three-dimensional* vortex street from the upstream cylinder on the downstream cylinder.

The photographs looking upstream (Figs. 9*a–c*) were taken from downstream of two cylinders in tandem, when the hydrogen bubbles were released upstream of the upstream cylinder, on a plane parallel to and 0.5D from the axis of the cylinders. The purpose was to examine the vortex-shedding phase along the span of the cylinder. The actual shape of the illuminated bubble sheet was dependent on the position at which it was released. As the hydrogen bubble wire was moved into the center of the cylinder, the "inner-wake" region was exposed, where mushroom-type structures similar to those shown in Fig. 7 were observed.

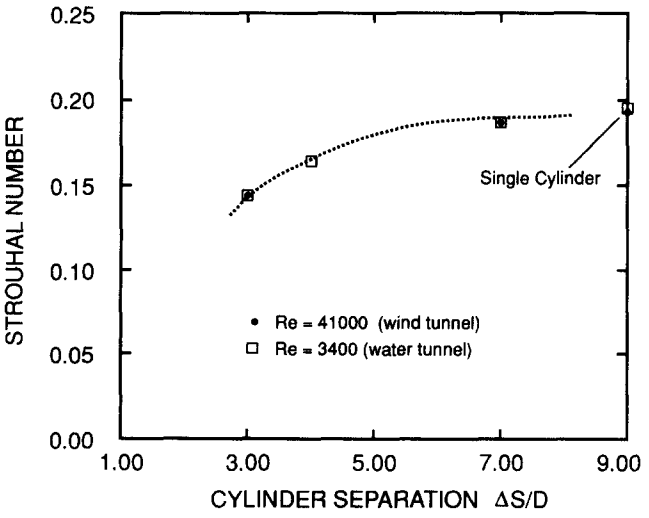

Figure 6. Variation of Strouhal number with cylinder separation; two cylinders in tandem.

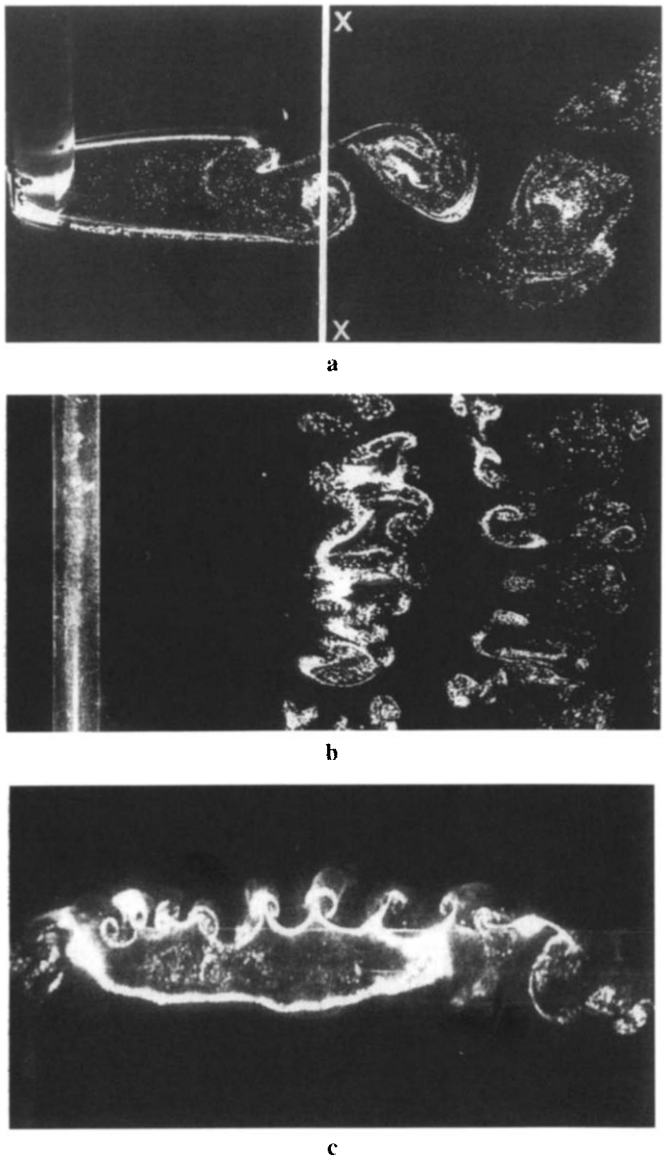

Figure 7. Water tunnel flow visualization of the wake behind a circular cylinder. D = 12 mm; Re = 1000. (*a*) End view; (*b*) side view; (*c*) upstream view. See also Fig. 1 for test setup.

Figure 9 shows the trends of increasing waviness when the separation distance, ΔS, between two cylinders was increased. This suggests that the vortex core was in phase for small separation distances; also there was significant phase shift along the span for large separation distances. This is entirely in agreement with the coherence data measured in the wind tunnel (Figs. 3*a*, *b*).

The distortion of the bubble line toward the ends of the cylinders in Fig. 9 was due to end effects where the cylinders meet the boundary layer of the walls of the working section. The visualization test was made using models with an aspect ratio, L/D, of 20.

Typical photographs showing the streamwise vortices embedded in the vortex of the two cylinders in tandem are shown in Figs. 10*a* and *b*. When the separation between cylinders was small, the development of streamwise vortices between the cylinders was suppressed and the

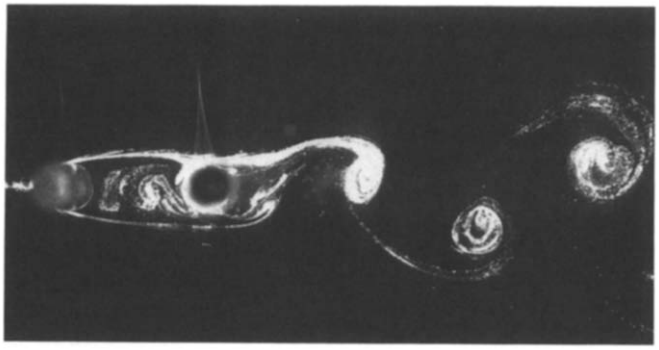

a

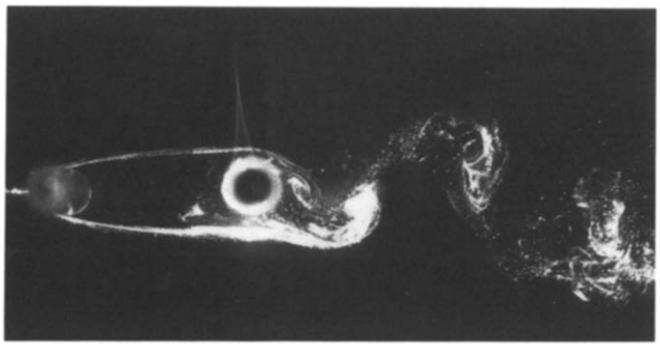

b

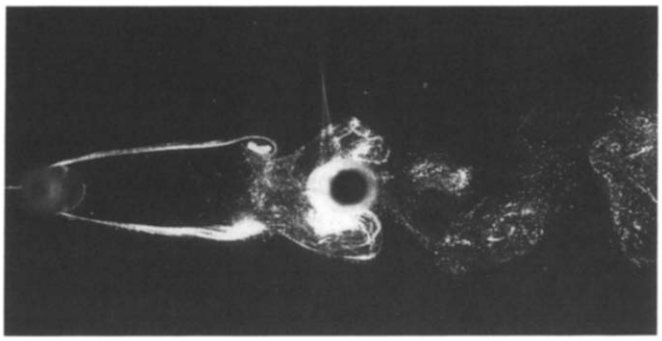

c

Figure 8. Flow visualization of two cylinders in tandem: end view, Re = 1000. Separation ΔS: (*a*) 3*D*; (*b*) 4*D*; (*c*) 6*D*.

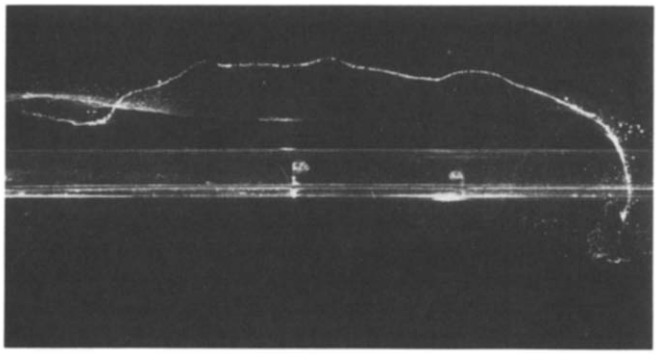

a

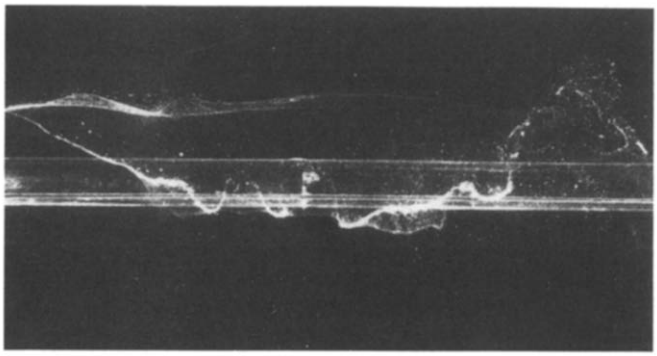

b

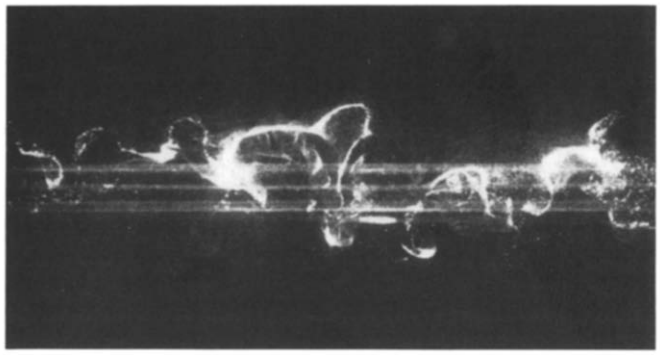

c

Figure 9. Flow visualization of two cylinders in tandem: upstream view, Re = 1000. Separation ΔS: (*a*) 3*D*; (*b*) 4*D*; (*c*) 6*D*.

streamwise vortices formed only behind the downstream cylinder (see Fig. 10*a*). At large separations between the cylinders, the formation of the Strouhal vortex between the two cylinders was accompanied by the development of streamwise vortices; the flow impinging on the downstream cylinder was highly three-dimensional.

DISCUSSION

Three-Dimensional Wake, Single Cylinder

The shedding of the Strouhal vortex has been known for many years. The formation of the Strouhal vortex results from nonlinear interactions of the two shear layers separating from the cylinder.

Grant [13] was perhaps the first to realize that the wake behind two-dimensional bluff bodies develops a three-dimensional structure. He used hot-wire anemometry and cross-correlation techniques to study the wake behind a cylinder and concluded that the Karman vortices develop a three-dimensional vortical structure composed of counterrotating streamwise vortices.

The early stages of the three-dimensional evolution of the streamwise vortices were investigated by Lasheras and Meiburg [14]. They simulated a plane wake behind a flat plate with a three-dimensional inviscid vortex method. Spanwise periodic perturbations were shown to grow into streamwise closed vortex loops connecting consecutive primary vortices, once the primary vortex was formed.

The mushroom-type structures in Figs. 7*b* and *c* are shear-aligned longitudinal votex tubes joining consecutive Strouhal vortices. The term "shear-aligned" means that the streamwise vortices align with the principal axis of the strain field of the Strouhal vortex. The vortex tubes are being stretched by the consecutive Strouhal vortices.

Cantwell and Coles [15] used a flying hot wire to measure the near-wake flow field behind a circular cylinder.

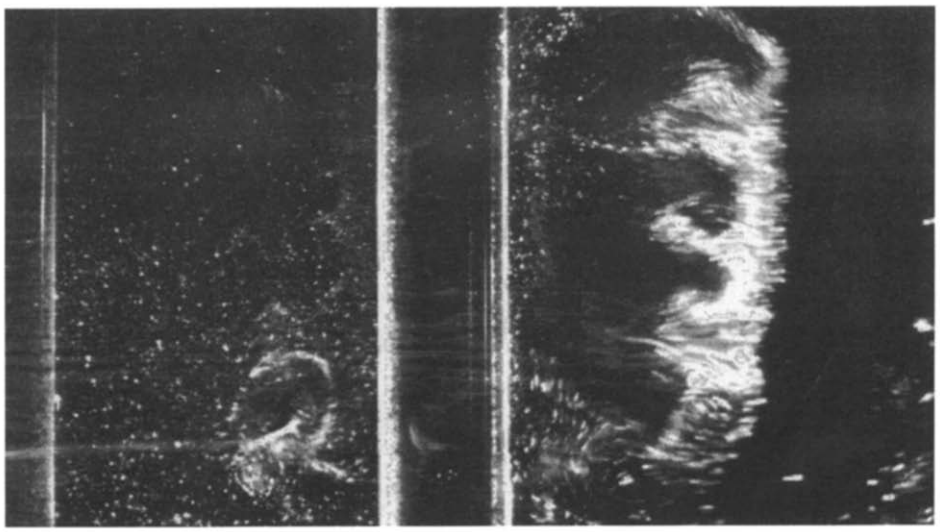

a

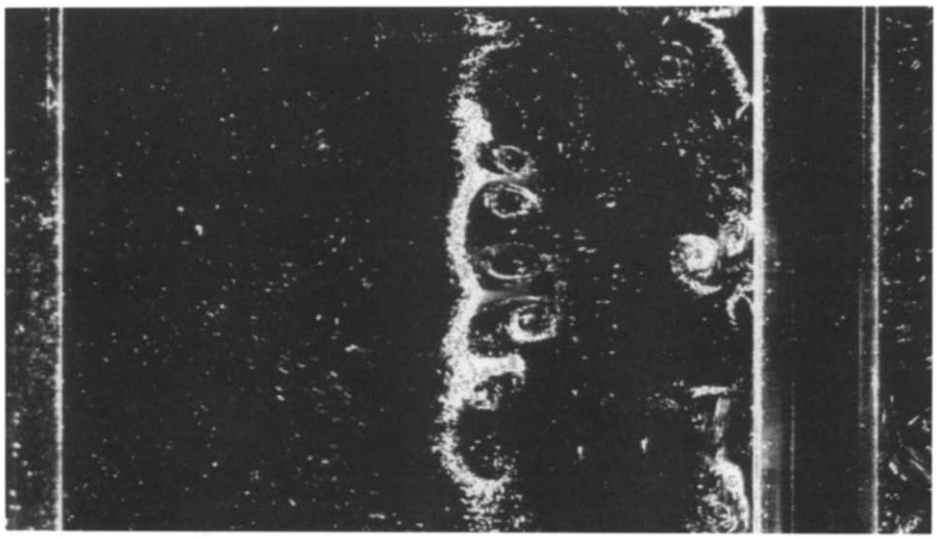

b

Figure 10. Streamwise vortices embedded in vortex street of two cylinders in tandem, Re = 1000. (*a*) Small separation, $\Delta S = 3.6D$, streamwise vortices formed only downstream of the second cylinder; (b) larger separation, $\Delta S = 6.6D$, streamwise vortices formed between the two cylinders.

One conclusion they drew was that a substantial part of the turbulence production is concentrated near the saddle points. It was conjectured that the turbulence production near saddles is carried out primarily by the stretching of small-scale vorticity oriented along the diverging separatrices.

The role of the streamwise vortices is therefore to produce the turbulence and hence three-dimensionality. This is one of the important mechanisms behind the decay of the coherence (or correlation) in the spanwise direction for the wake behind a single cylinder (see Fig. 3*a*). This mechanism also contributes to a sharp reduction in the spanwise coherence in the wake of two cylinders in tandem when the separation between them is large.

It is estimated that the ratio of the spanwise wavelength of the mushroom-type structures to the streamwise wavelength of the Strouhal vortex is about 0.5 at Re = 1000. Both the structure and the ratio are similar to the braid in plane mixing layers [16]. Similar braid structures have also been identified in the near-wake region behind a cylinder in very low Reynolds number flow, that is, for Re < 400 [17].

Three-Dimensional Wake, Two Cylinders in Tandem

The flow interference of the two circular cylinders in tandem has been reviewed by Zdravkovich [18], who showed that a discontinuity exists at a critical spacing, due to the discontinuity in the vortex-shedding pattern. He noticed that the drag coefficient changes abruptly at a spacing of approximately $3D$. These are all reflected in our spanwise coherence measurements behind the upstream cylinder (Fig. 4) and behind the downstream cylinder (Fig. 3). The spanwise coherence of the wake behind the upstream cylinder was not influenced by the second cylinder if the spacing was greater than $4D$. However, when the separation was reduced to $3D$, a large increase in coherence of the upstream cylinder was recorded (Figs. 4*a*, *b*).

When two cylinders are placed in tandem, the wake

from the upstream cylinder introduces a velocity perturbation that interacts with the downstream cylinder. The level and form of this perturbation depends on the distance between the cylinders. The formation of the vortex structures and the magnitude of the spanwise coherence will depend on the separation distance and the Reynolds number.

When two cylinders are close together (e.g., separated by $3D$) there is insufficient time or space for the development of the Strouhal vortex behind the upstream cylinder. The downstream cylinder acts to suppress the shedding of the upstream vortex. The streamwise vortices are also suppressed, as shown in Fig. 10*a*. The turbulence intensity and flow three-dimensionalities of the impinging flow on the downstream cylinder are weak. The spanwise jitter of the vortex shed from the downstream cylinder is small. High spanwise coherence is therefore expected (see Fig. 3).

Similar results were obtained by Arie et al [1]. They measured the surface pressure signal over a range of circumferential positions of two cylinders in tandem for different spanwise separations. The pressure signals measured at 90° and 110° from the upstream stagnation point are indicative of the vortex-shedding process. The correlation length they obtained at these locations of the downstream cylinder shows a continuing increase when the separation distance is reduced.

It is rather surprising to note that at sufficiently small separation (e.g., $3D$) the spanwise coherence becomes greater than that of the single cylinder. It was observed that although the vortex shed from the upstream cylinder was suppressed at the Separation of $3D$, the oscillation of the shedding signal from the wake of the second cylinder could still be detected in between the two cylinders. A peak at the shedding frequency in the velocity power spectrum was observed during the experiment when the hot-wire probe was placed in the separating shear layer behind the upstream cylinder. This indicates a response of the separating shear layers behind the upstream cylinder to the upstream-propagating wave of the oscillating velocity field of the vortex street behind the downstream cylinder. Obviously, the oscillating shear layers from the upstream cylinder impinging on the downstream cylinder will influence the initiation of the vortex street of the downstream cylinder. It is therefore conjectured that some form of a feedback loop is established that is responsible for the measured higher spanwise coherence.

For large separations between the cylinders in tandem, the formation of the vortex from the upstream cylinder results in a high level of turbulence upstream of the second cylinder and there is a sharp reduction of coherence with spanwise separation (Fig. 3). This is in agreement with the findings of Kiya et al [2], who found that high upstream turbulence reduces spanwise coherence. The streamwise vortices embedded in the Strouhal vortex from the upstream cylinder introduce strong three-dimensionalities and random perturbations in the initiation of the vortex of the second cylinder. This is also one of the important mechanisms for the sharp reduction in spanwise coherence at large separations; at a separation of $12D$, the spanwise coherence is an order of magnitude smaller than that of the single cylinder (Fig. 3).

The Reynolds number at which the flow visualization experiments were carried out was low due to the difficulties of recording images in high-speed flow. This means that vortex structures might not be identical for those measured from the wind tunnel tests and those from water tunnel visualization. However, the fluid dynamic process revealed by the flow visualization showed trends similar to those of the wind tunnel results.

PRACTICAL SIGNIFICANCE

There are numerous examples of flow past cylinders (e.g., chimney stacks, electric transmission lines) of varying size and spacing. Our particular interest is the instantaneous forced convection process with a view to augmenting heat transfer in cross-flow heat exchangers for a minimum increase in pressure loss. An understanding of the fluid dynamics involved will contribute directly to the achievement of this goal.

SUMMARY

The wake behind a cylinder develops counterrotating pairs of riblike longitudinal vortex structures. These structures appear to be responsible for the high degree of three-dimensionality in the near wake, which results in the decay of the spanwise coherence of the fluctuating velocities.

When two cylinders are placed in tandem, the distance between the cylinders has a strong influence on the form and development of the wake of the downstream cylinder. If the separation distance is small (e.g., less than three cylinder diameters), the vortex shedding from the upstream cylinder is suppressed by the second cylinder, and the spanwise coherence (correlation) is higher and shedding frequency is lower than those corresponding to a single cylinder. If the separation distance is large (e.g., $> 4D$), there is sufficient space between the cylinders for the development of a three-dimensional vortex wake behind the upstream cylinder, and the flow impinging on the downstream cylinder has a high level of turbulence and three-dimensionality (due to the streamwise vortices). This reduces the spanwise coherence of the wake behind the downstream cylinder; the spanwise correlation of the wake falls almost to zero when the cylinders are $12D$ apart.

RECOMMENDATION FOR FUTURE WORK

While there are extensive data of body surface pressure measurement for two cylinders in tandem, quantitative flow-field data describing the spanwise fluid structures are still limited. It is recommended that future efforts be directed toward multipoint spanwise velocity field measurement. A technique such as particle image velocimetry (PIV) could be used to obtain the instantaneous whole-field flow structures.

We wish to thank Mr. N. Hamilton for the photographs presented in this article.

NOMENCLATURE

coh	coherence function, dimensionless
D	diameter of cylinder, mm
G	Fourier transform of fluctuating velocity, dimensionless

L spanwise length of model, mm
L_y longitudinal integral scale of free-stream turbulence, mm
Re Reynolds number ($= U_\infty D/\nu$), dimensionless
St Strouhal number ($= fD/U_\infty$), dimensionless
T Taylor number $\{= [(\overline{u^2})^{0.5}/U_\infty](D/L_y)^{0.2}\}$ dimensionless
Z spanwise coordinate, mm
U_∞ free-stream velocity, m/s

Greek Symbols

ΔS distance between cylinder centers in flow direction, mm
ΔZ spanwise separation of the hot-wire probes, mm
ω frequency variable in fourier space, Hz

REFERENCES

1. Arie, M., Kiya, M., Moriya, M., and Mori, H., Pressure Fluctuations on the Surface of Two Circular Cylinders in Tandem Arrangement, *J. Fluids Eng.* **105,** 161–167, 1983.
2. Kiya, M., Suzuki, Y., Arie, M., and Hagino, M., A Contribution to the Free-stream Turbulence Effect on the Flow Past a Circular Cylinder, *J. Fluid Mech.* **115,** 151–164, 1982.
3. Ramberg, S. E., and Griffin, O. M., Velocity Correlation and Vortex Spacing in the Wake of a Vibrating Cable, *ASME J. Fluids Eng.* 10–18, March 1976.
4. Sarpkaya, T., Vortex Induced Oscillations: A Selective Review, *J. Appl. Mech.* **46,** 241–258, June 1979.
5. Ferre, J. A., Mumford, J. C., Savill, A. M., and Giralt, F., Three-Dimensional Large-Eddy Motions and Fine-Scale Activity in a Plane Turbulent Wake, *J. Fluid Mech.* **210,** 371–414, 1990.
6. Hayakawa, H., and Hussain, A. K. M. F., Three-Dimensionality of Organized Structures in a Plane Turbulent Wake, *J. Fluid Mech.* **206,** 375–404, 1989.
7. Welch, L. W., Wu, J., Walker, G. J., and Hamilton, N. B., Three-Dimensional Near-Field Wakes Downstream of a Circular Cylinder and Two Cylinders in Tandem, 2nd World Conf. on Exp. Heat Transfer, Fluid Mech. and Thermodynamics, Dubrovnik, Yugoslavia, 186–193, June 23–28, 1991.
8. Welsh, M. C., Soria, J., Sheridan, J., Wu, J., Hourigan, K., and Hamilton, N., Three-Dimensional Flows in the Wake of a Circular Cylinder, *Visualization Soc. Jpn.* **9,** 17–18, 1992.
9. Wu, J., Soria, J., Sheridan, J., and Welsh, M. C., Identification of Vortex Structures in Plane Wakes Using Digital Image Methods, IUTAM Symp. on Eddy Structure Identification in Free Turbulent Shear Flows, Poitiers, France, XI.10.1–10.5, Oct. 14–16, 1992.
10. Stokes, A. N., and Welsh, M. C., Flow-Resonant Sound Interaction in a Duct Containing a Plate, *J. Sound Vib.* **104,** 55–73, 1986.
11. Toebes, G. H., The Unsteady Flow and Wake Near an Oscillating Cylinder, *ASME J. Basic Eng.* **91**(3), 493–505, 1969.
12. Bull, M. K., Pickles, J. M., Martin, B. T., and Welsh, M. C., Vortex Shedding from Rectangular Plates in Tandem, 10th Australasian Fluid Mechanics Conf., Melbourne, **I,** 4.17–4.20, Dec. 11–15, 1989.
13. Grant, M. L., The Large Eddies of Turbulent Motion, *J. Fluid Mech.* **4,** 149–190, 1958.
14. Lasheras, J. C., and Meiburg, E., Three-Dimensional Vorticity Modes in the Wake of a Flat Plate, *Phys, Fluids* **A2**(3), 371–380, 1990.
15. Cantwell, B., and Coles, D., An Experimental Study of Entrainment and Transport in the Turbulent Near Wake of a Circular Cylinder, *J. Fluid Mech.* **136,** 321–374, 1983.
16. Bernal, L. P., and Roshko, A., Streamwise Vortex Structure in Plane Mixing Layers, *J. Fluid Mech.* **170,** 499–525, 1986.
17. Williamson, C. H. K., The Existence of Two Stages in the Transition to Three-Dimensionality of a Cylinder Wake, *Phys. Fluids* **31**(11), 3165–3168, 1988.
18. Zdravkovich, M. M., Review of Flow Interference Between Two Circular Cylinders in Various Arrangements, *ASME J. Fluids Eng.* **99,** 618–633, 1977.

Received April 19, 1993; revised April 11, 1994